# Mechanistic Investigations on the Hydrogenation of Alkenes Using Ruthenium(II)-arene Diphosphine Complexes

Corinne Daguenet, Rosario Scopelliti, and Paul J. Dyson*

*Institut des Sciences et Ingénierie Chimiques, Ecole Polytechnique Fédérale de Lausanne, EPFL-BCH, CH-1015 Lausanne, Switzerland*

*Received May 12, 2004*

The ruthenium(II) complexes [Ru($\eta^2$-P−P)($\eta^6$-*p*-cymene)Cl]Cl, P−P = diphenylphosphinomethane (dppm), diphenylphosphinoethane (dppe), or diphenylphosphinopropane (dppp), and the highly water-soluble analogues, [Ru($\eta^2$-P−P)($\eta^6$-arene)Cl]$Na_3$, P−P = 1,2-bis(di-4-sulfonatophenylphosphino)benzene (dppbts), arene = *p*-cymene, benzene, or [2.2]paracyclophane, are efficient catalyst precursors for the hydrogenation of styrene in an aqueous biphase. By the use of high gas pressure NMR techniques and electrospay ionization mass spectrometry, the active species in the hydrogenation have been indirectly identified to be a dihydrogen complex, which also catalyzes H/D isotope exchange. Using the ruthenium(II) dppbts derivatives as precatalysts, evidence is provided for an arene exchange process that takes place during the catalytic hydrogenation of styrene. Together, these results lead to the proposition of a catalytic cycle for the hydrogenation of the C=C double bond of styrene using ruthenium(II)-arene diphosphine complexes.

## Introduction

To improve product separation and catalyst recycling using molecular (homogeneous) species, the use of biphasic conditions has emerged as a judicious solution, especially with the environmentally friendly aqueous biphase,[1−3] although supercritical fluids,[4] ionic liquids,[5] and fluorous processes[6] are also being evaluated. The use of water in biphasic catalysis not only derives from its benign nature but is also an easily tuneable medium, which provides many unique opportunities in catalysis.[7,8] A large number of catalysts have been investigated in water, including many hydrogenation catalysts.[1,8]

The catalytic hydrogenation of the C=C bonds by ruthenium(II) complexes has been widely reported, and while the majority of catalysts operate under homogeneous conditions,[9−13] aqueous biphasic conditions have been applied,[14−16] in which hydrophilic ligands are employed to induce water solubility of the catalysts. The mechanism of hydrogenation reactions involving ruthenium(II) complexes is thought, in most cases, to operate via the so-called "hydride" route, as do, for example, the well-known complex [$RuCl_2(PPh_3)_3$] and the arene dimer [$RuCl_2$(arene)]$_2$, which react under hydrogen to form active hydride species by loss of HCl.[9,17] Other ruthenium(II) complexes such as [Ru($O_2CCH_3)_2$(arene)] and [Ru($O_2CCH_3)_2$(diphosphine)] also heterolytically cleave $H_2$ to give active hydride species.[17−19] In addition to the hydride route a few groups have postulated that hydrogen transfer could directly occur from a dihydrogen complex, as in the case with the dimeric species [Ru(diphosphine)$Cl_2]_2$, which binds $H_2$ to form the triply bridged chloro complex [Ru(diphosphine)($\eta^2$-$H_2$)($\mu$-Cl)$_3$-RuCl(diphosphine)].[20] Here the hydrogen can transfer to a $\pi$-bonded alkene. With the arene ruthenium(II) complex [Ru($CH_3CN)_3$(benzene)][$BF_4]_2$, which operates in an aqueous biphase, both the hydride and dihydrogen routes have been proposed.[21]

While these mechanistic studies were conducted in organic solvent, with the exception of the latter example, it is also possible to study catalyst reaction mechanisms in aqueous−organic biphasic processes.[21−23]

(1) Joó, F. *Aqueous Organometallic Catalysis*; Kluwer: Dordrecht, 2001.
(2) Cornils, B., Herrmann, W. A., Eds. *Aqueous-Phase Organometallic Catalysis. Concepts and Applications*; Wiley-VCH: Weinheim, 1998.
(3) Joó, F.; Papp, É.; Kathó, Á. *Top. Catal.* **1998**, *5*, 113.
(4) Jessop, P. G.; Leitner, W. *Chemical Synthesis using Supercritical Fluids;* Wiley-VCH, Weinheim, 1999.
(5) Dupont, J.; D. Souza, R. F.; Suarez, P. A. Z. *Chem. Rev.* **2002**, *102*, 3667.
(6) Horváth, I. T. *Acc. Chem. Res.* **1998**, *31*, 641.
(7) Joó, F.; Kovács, J.; Bényei, A. Cs.; Kathó, Á. *Angew. Chem., Int. Ed.* **1998**, *37*, 969.
(8) Joó, F. *Acc. Chem. Res.* **2002**, *35*, 738.
(9) James, B. R. *Homogeneous Hydrogenation*; Wiley: New York, 1973.
(10) Halpern, J.; Harrod, J. F.; James, B. R. *J. Am. Chem. Soc.* **1966**, *88*, 5150.
(11) Hallman, P. S.; Evans, D.; Osborn, J. A.; Wilkinson, G. *Chem. Comm.* **1967**, *7*, 305.
(12) Suarez, T.; Fontal, B. *J. Mol. Catal.* **1988**, *45*, 335.
(13) Corma, A.; Iglesias, M.; Del Pino, C.; Sanchez, F. *J. Organomet. Chem.* **1992**, *431*, 233.
(14) Andriollo, A.; Bolívar, A.; López, F. A.; Páez, D. E. *Inorg. Chim. Acta* **1995**, *238*, 187.
(15) Ellis, D. J.; Dyson, P. J.; Parker, D. G.; Welton, T. *J. Mol. Catal. A* **1999**, *150*, 71.
(16) )Rojas, I.; Linares, F. L.; Valencia, N.; Bianchini, C. *J. Mol. Catal. A* **1999**, *144*, 1.
(17) Brothers, P. J. *Prog. Inorg. Chem.* **1981**, *28*, 1.
(18) Ashby, M. T.; Halpern, J. *J. Am. Chem. Soc.* **1991**, *113*, 589.
(19) Bennett, M. A.; Ennett, J. P. *Inorg. Chim. Acta* **1992**, *198−200*, 583.
(20) Joshi, A. M.; MacFarlane, K. S.; James, B. R. *J. Organomet. Chem.* **1995**, *488*, 161.
(21) Chan, W.-C.; Lau, C.-P.; Cheng, L.; Leung, Y.-S. *J. Organomet. Chem.* **1994**, *464*, 103.

10.1021/om049665q CCC: $27.50 
Publication on Web 09/09/2004

**Chart 1**

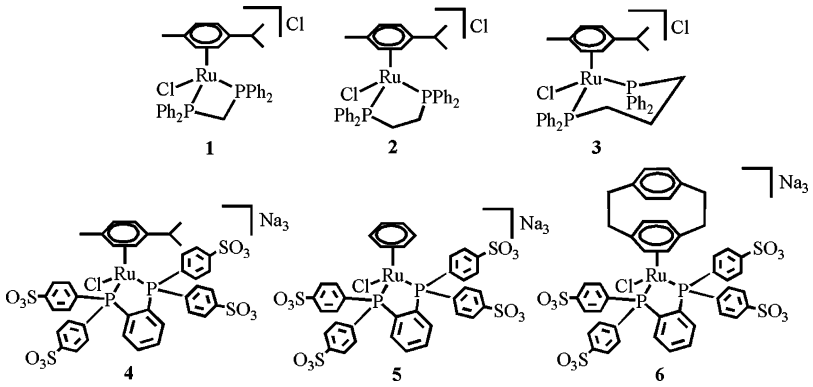


In this work, we report the use of ruthenium(II)-arene diphosphine complexes as precatalysts for the hydrogenation of styrene, including water-soluble complexes that operate in an aqueous biphase. Remarkably, the biphasic conditions provide a way to study the evolution of the various species present after catalysis employing in particular electrospray ionization mass spectrometry (ESI-MS), which has been previously shown to be an efficient technique to observe transition metal complexes.[24] In addition, high gas pressure NMR spectroscopy[25] gives further clues to the mechanism.

## Results and Discussion

A series of ruthenium(II)-arene diphosphine complexes have been synthesized from the appropriate dimer, [{Ru($\eta^6$-arene)$Cl_2$}$_2$] (Chart 1). The complexes [Ru(diphosphine)($\eta^6$-*p*-cymene)Cl]Cl, diphosphine = diphenylphosphinomethane (dppm) (**1**), diphenylphosphinoethane (dppe) (**2**), or diphenylphosphinopropane (dppp) (**3**), were prepared according to a method described by Faraone et al. with some modifications.[26] In our experience, the literature procedure results in the formation of byproducts including phosphine-bridged bimetallic complexes and bis-diphosphine species resulting from arene displacement, as noted elsewhere.[27] To avoid bridged species, a large excess of diphosphine was used and lower temperatures were applied to prevent loss of the arene. In this way, the cationic diphosphine complexes were formed as the main species with chloride as the counteranion. The chloride is easily replaced with tetrafluoroborate in aqueous solution. NMR data for these complexes were in accordance with the literature data.[28] To preclude side-reactions, another route has also been developed, but it involves a supplementary step, that is, the formation of [Ru($\eta^6$-arene)-($CH_3CN$)$_2$Cl][$PF_6$].[27,28]

Using an adaptation of the above method, the water-soluble diphosphine 1,2-bis(di-*p*-sulfonatophenylphosphino)benzene (dppbts) was reacted with three different dimers to afford [Ru($\eta^6$-arene)(dppbts)Cl]$Na_3$ (arene = *p*-cymene (**4**), benzene (**5**), or [2.2]paracyclophane (**6**)). Direct reaction of the dimer with dppbts in a mixture of water−ethanol (1:1) for a much shorter period of time, followed by precipitation of the complex after addition of ethanol, affords **4**−**6** in moderate to good yield.

The electrospray ionization (ESI) mass spectra of **4**, **5**, and **6** in water, recorded in negative ion mode, show strong peak envelopes corresponding to the triply charged anion [Ru(dppbts)($\eta^6$-arene)Cl]$^{3-}$ ([M]$^{3-}$), centered at $m/z$ = 344.3, 325.7, and 369.0, respectively. Less intense peaks, which correspond to species with a countercation, [M + H]$^{2-}$ and [M + Na]$^{2-}$, are also observed at $m/z$ = 516.9 and 527.8 for **4**, 489.0 and 499.9 for **5**, and 554.0 and 565.0 for **6**; these data are in keeping with those observed for other sulfonated phosphine complexes.[29] The $^{31}$P NMR spectra of these complexes in methanol-$d_4$ exhibit singlets at $\delta$ 67.1 for **4**, $\delta$ 65.1 for **5**, and $\delta$ 72.9 for **6**, which is consistent with the ring contribution of a five-membered ring formed by chelation.[30] Confirmation of the identity of **4**−**6** was provided by two-dimensional $^{13}$C−$^{1}$H correlation NMR spectroscopy in methanol-$d_4$ (see Supporting Information for full details). Cross-peaks, characteristic of the $\eta^6$-coordinated arenes, appear at $\delta$ 6.27 and $\delta$ 98.09, 93.64 for **4**, $\delta$ 6.22 and $\delta$ 97.80 for **5**, and $\delta$ 5.21 and $\delta$ 94.68 for **6**, in the $^{1}$H and $^{13}$C dimensions, respectively. Compounds **4**−**6** contain approximately 10% dppbts dioxide with a characteristic $^{31}$P NMR signal at ca. $\delta$ 33.2 in methanol-$d_4$. A small amount of the hydride [Ru(dppbts)($\eta^6$-arene)H]$^{3-}$ is detected by negative ion ESI-MS in **5** and **6** [$m/z$ = 314.3 and 357.9, respectively], as well as the hydrolysis product, [Ru(dppbts)($\eta^6$-arene)-($H_2O$)]$^{2-}$ [$m/z$ = 480.0 for **5** and 545.0 for **6**].

The structures of **1**·$BF_4$ and **2**·$BF_4$ were established by single-crystal X-ray diffraction in order to ascertain the P−Ru−P angle and correlate this bite angle with the kinetics of hydrogenation (see below, Table 2). X-ray suitable crystals of the two tetrafluoroborate salts were obtained by slow evaporation from acetone, and the resulting structures of **1**·$BF_4$ and **2**·$BF_4$ are depicted in Figures 1 and 2, respectively, with key bond parameters listed in the captions. The two structures are similar to related ruthenium-arene diphosphine structures that have been published previously.[31,32]

(22) Ogo, S.; Abura, T.; Watanabe, Y. *Organometallics* **2002**, *21*, 2964.
(23) Jayasree, S.; Seayad, A.; Sarkar, B. R.; Chaudhari, R. V. *J. Mol. Catal. A* **2002**, *181*, 221.
(24) Dyson, P. J.; McIndoe, J. S. *Inorg. Chim. Acta* **2003**, *354*, 68.
(25) Elsevier: C. J. *J. Mol. Catal.* **1994**, *92*, 285.
(26) Faraone, F.; Loprete, G. A.; Tresoldi, G. *Inorg. Chim. Acta* **1979**, *34*, L251.
(27) Fogg, D.; James, B. R. *J. Organomet. Chem.* **1993**, *462*, C21.
(28) Jensen, S. B.; Rodger, S. J.; Spicer, M. D. *J. Organomet. Chem.* **1998**, *556*, 151.
(29) Bryce, D. J. F.; Dyson, P. J.; Nicholson, B. K.; Parker, D. G. *Polyhedron* **1998**, *17*, 2899
(30) Garrou, P. E. *Chem. Rev.* **1981**, *81*, 229.
(31) De los Rios, I.; Jiménez Tenorio, M.; Jiménez Tenorio, M. A.; Puerta, M. C.; Valerga, P. *J. Organomet. Chem.* **1996**, *525*, 57.

**Table 1. Crystal Data and Details of the Structure Determination for 1·$BF_4$ and 2·$BF_4$**

| | 1·$BF_4$ | 2·$BF_4$ |
|---|---|---|
| chemical formula | $C_{35}H_{36}BClF_4P_2Ru$ | $C_{36}H_{38}BClF_4P_2Ru$ |
| fw | 741.91 | 755.93 |
| cryst syst | orthorhombic | orthorhombic |
| space group | $P2_12_12_1$ | $P2_12_12_1$ |
| $a$ (Å) | 11.861(5) | 12.4176(6) |
| $b$ (Å) | 15.411(5) | 15.2102(7) |
| $c$ (Å) | 18.360(3) | 17.3187(10) |
| volume (Å$^3$) | 3356.1(18) | 3271.0(3) |
| $Z$ | 4 | 4 |
| $D_{calc}$ (g cm$^{-3}$) | 1.468 | 1.535 |
| $F$(000) | 1512 | 1544 |
| $\mu$ (mm$^{-1}$) | 0.688 | 0.708 |
| temp (K) | 293(2) | 140(2) |
| wavelength (Å) | 0.71070 | 0.71073 |
| measd reflns | 20 159 | 20 135 |
| unique reflns | 5883 | 5750 |
| unique reflns [$I > 2\sigma(I)$] | 4216 | 5351 |
| no. of data/params | 5883/430 | 5750/406 |
| $R^a$ [$I > 2\sigma(I)$] | 0.0405 | 0.0275 |
| wR2$^a$ (all data) | 0.0978 | 0.0601 |
| GoF$^b$ | 0.956 | 1.032 |

$^a$ $R = \sum||F_o| - |F_c||/\sum|F_o|$, $wR2 = \{\sum[w(F_o^2 - F_c^2)^2]/\sum[w(F_o^2)^2]\}^{1/2}$. $^b$ GoF $= \{\sum[w(F_o^2 - F_c^2)^2]/(n - p)\}^{1/2}$ where $n$ is the number of data and $p$ is the number of parameters refined.

**Table 2. Effect of the Steric Constraints of [Ru(*p*-cymene)(P−P)Cl]Cl on the Initial Rate of Styrene Hydrogenation$^a$**

| P−P | bite angle/deg | $v_0$/M min$^{-1}$ |
|---|---|---|
| dppm | 71.3$^b$ | 0.125 ± 0.013 |
| dppe | 83.0$^b$ | 0.377 ± 0.017 |
| dppp | 91.1$^c$ | 4.2 ± 0.9 |

$^a$ Reaction conditions: 80 °C, $p(H_2) = 45$ bar, substrate/catalyst = 1500, in toluene-$d_8$. $^b$ This work, $^c$ Estimation from ref 40.

**Catalytic Investigations.** Compounds **1**−**6** were tested for catalytic hydrogenation of styrene with molecular hydrogen in order to assess their activity. Using toluene as a cosolvent with complexes **1**−**3**, in an autoclave at 100 °C and at a partial pressure of hydrogen of 45 bar with a ratio substrate/catalyst of about 2000, 100% conversion was observed when the reaction is stopped after 2 h, which provides a high turnover frequency (TOF) compared to other related ruthenium complexes.[33−36] Similar activities are observed in an aqueous biphase under the same conditions. Addition of mercury, as a selective poison for colloidal/nanoparticle catalysts,[37] does not affect the conversion, neither in a pure organic phase nor under biphasic conditions, indicating that the active catalyst is homogeneous.

Hydrogenations using **1**−**3** were also performed in deuterated toluene in a sapphire NMR tube[38] and monitored by $^1$H NMR spectroscopy (Figure 3, A). Initial rates were determined for each diphosphine complex (Table 2). A trend is observed showing an enhancement of the initial rate with the increase of the alkyl chain length of the diphosphine. Progressing from dppm to dppp, the P−Ru−P bite angle becomes larger, increasing the steric constraints around the coordination sphere of the metal. The bite angles of diphosphines have previously been shown to effect the catalytic activity and selectivity of several important reactions.[39,40] In the system described herein, the correlation of the bite angle with the activity is consistent with a dissociative process occurring during a rate-determining step. Dissociation of the coordinated chloride to give a dihydrogen complex (or dihydride) is then postulated.

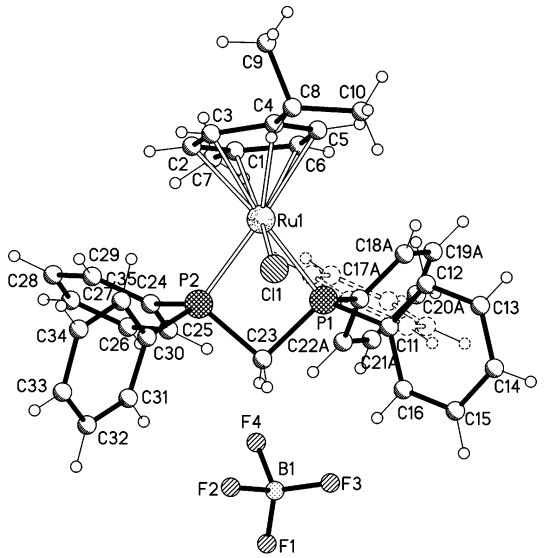


**Figure 1.** Ball-and-stick representation of the crystal structure of **1**·$BF_4$. Selected bond distances (Å) and angles (deg): Ru1−Cl1, 2.397(2); Ru1−P1, 2.316(2); Ru1−P2, 2.309(2); P1...P2, 2.695(3); P1−Ru1−P2, 71.29(6); Cl1−Ru1−P1, 83.47(5); Cl1−Ru1−P2, 84.25(6); P1−C23−P2, 95.3(3).

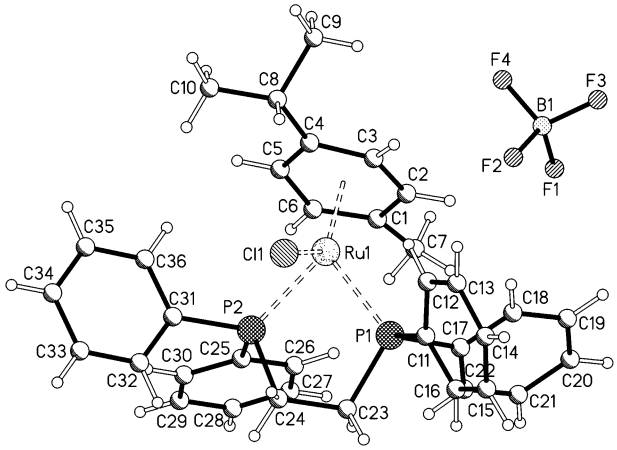


**Figure 2.** Ball-and-stick representation of the crystal structure of **2**·$BF_4$. Selected bond distances (Å) and angles (deg): Ru1−Cl1, 2.430(1); Ru1−P1, 2.329(1); Ru1−P2, 2.336(1); P1...P2, 3.092(2); P1−Ru1−P2, 83.03(3); Cl1−Ru1−P1, 89.43(5); Cl1−Ru1−P2, 80.87(3).

(32) Mashima, K.; Kusano, K.; Ohta, T.; Noyori, R.; Takaya, H. *J. Chem. Soc., Chem. Commun.* **1989**, 1208.
(33) Moldes, I.; de la Encarnación, E.; Ros, J.; Alvarez-Larena, Á.; Piniella, J. F. *J. Organomet. Chem.* **1998**, *566*, 165.
(34) Parmar, D. U.; Bhatt, S. D.; Bajaj, H. C.; Jasra, R. V. *J. Mol. Catal. A* **2003**, *202*, 9.
(35) Baricelli, P. J.; Rodríguez, G.; Rodríguez, M.; Lujano, E.; López-Linares, F. *Appl. Catal. A* **2003**, *239*, 25.
(36) Baricelli, P. J.; Izaguirre, L.; López, J.; Lujano, E.; López-Linares, F. *J. Mol. Catal. A* **2004**, *208*, 67.
(37) Whitesides, G. M.; Hackett, M.; Brainard, R. L.; Lavalleye, J.-P. P. M.; Sowinski, A. F.; Izumi, A. N.; Moore, S. S.; Brown, D. W.; Staudt, E. M. *Organometallics* **1985**, *4*, 1819.
(38) Cusanelli, A.; Frey, U.; Richens, D. T.; Merbach, A. E. *J. Am. Chem. Soc.* **1996**, *118*, 5265.
(39) Subongkoj, S.; Lange, S.; Chen, W.; Xiao, J. *J. Mol. Catal. A* **2003**, *196*, 125.
(40) Dierkes, P.; van Leeuwen, P. W. N. M. *J. Chem. Soc., Dalton Trans.* **1999**, 1519.

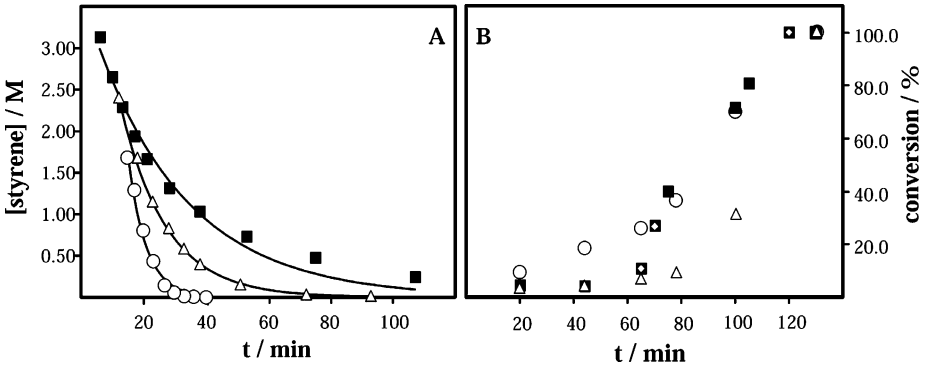


**Figure 3.** Influence of the diphosphine on the rate of styrene hydrogenation using **1**−**3** as catalyst precursors: **1** (solid squares), **2** (empty triangles), **3** (empty circles). (A) Homogeneous organic phase. Concentrations were determined by in situ high-pressure $^1$H NMR spectroscopy by integration of the signals at long relaxation delay. Data was fitted using a monoexponential (straight lines). Reaction conditions: 80 °C, $p(H_2) = 45$ bar, substrate/catalyst = 1500, in toluene-$d_8$. (B) Aqueous biphase. Conversions were determined by GC analysis after reaction in an autoclave, addition of mercury with **1** (empty diamonds). Conditions: 100 °C, $p(H_2) = 45$ bar, substrate/catalyst = 2000, in water.

The kinetics of hydrogenation with **1**−**3** under biphasic conditions does not follow the same behavior as those observed under homogeneous conditions (Figure 3, B). In fact, an induction period is observed showing that additional factors influence the reaction. The bite angle effect is presumably counterbalanced by other phenomena including differences in solubility of the complexes in water as well as phase transfer of the complexes into the organic layer. Indeed, after biphasic hydrogenation, the organic phase is colored, indicating contamination by the complexes and limiting their utility in biphasic catalysis. A mechanistic study is not feasible since the $^{31}$P NMR spectrum of the organic phase recorded after catalysis is complicated and the presence of free *p*-cymene is detected in the $^1$H NMR spectrum.

To delineate the differences between the aqueous-biphase and homogeneous organic systems, dppbts derivatives were used to immobilize the ruthenium(II)-arene complexes in water. Thus, complexes **4**−**6** were evaluated as catalysts for hydrogenation of styrene in water. Under the same conditions as those mentioned above, 100% conversion to ethylbenzene as the only product was observed for each compound after 2 h. Poisoning experiments with mercury were performed, and the activity of complexes **4**−**6** was completely suppressed. However, it is known that mercury can sometimes also react with a single-metal complex and deactivate the catalyst, leading then to an ambiguous conclusion.[41,42] In the present case, the sulfonate groups might be responsible for this interaction since they have been reported to adsorb on mercury.[43] Furthermore, below pH 3, catalysis is inhibited; in this pH range, the first protonation of a sulfonate group could partially occur and deactivate the complex. Indeed, at pH < 2, the protonated complex $[M + H]^{2-}$ is the only ruthenium species observed on the ESI mass spectrum of **4**, and although the proton affinity in the gas phase does not exactly reflect the one in solution, it is reasonable to assume that protonation is still taking place to some extent in the aqueous phase. These elements indicate

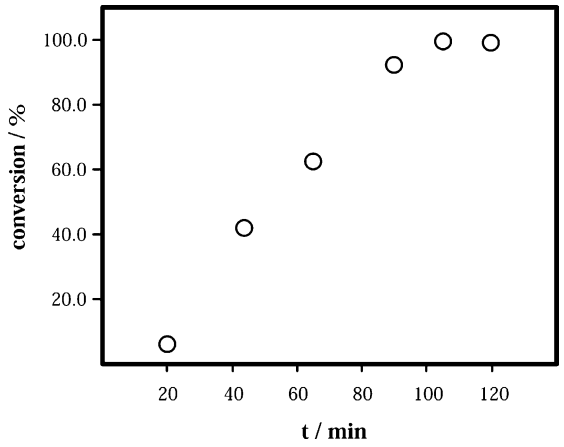


**Figure 4.** Kinetics of styrene hydrogenation using **4** as the catalyst precursor. Conversions determined by GC analysis. Conditions: 100 °C, $p(H_2) = 45$ bar, substrate/catalyst = 2000, styrene (1 mL), $H_2O$ (1.5 mL).

that sulfonate groups participate in catalytic activity, possibly by increasing the solubility of styrene in water.

The behavior of the kinetics for the hydrogenation of styrene with **4** under biphasic conditions is presented in Figure 4. An induction period of ca. 20 min is observed, which might correspond to the formation of an active catalytic species. The kinetics are then defined by an essentially linear trend, probably because of the low solubility of styrene in water, which provides a constant concentration until almost all the substrate is converted to ethylbenzene. Considering the concentration of styrene as a limiting factor, giving rise to a zero-order dependence, it seems likely that the reaction is taking place in the water bulk.

The catalytic hydrogenation performed with **6** results in 100% conversion of the substrate even after 1 h of reaction, demonstrating a higher activity for the [2.2]-paracyclophane derivative, which will be discussed later on.

ESI-MS was used to analyze the aqueous phase after catalysis; previously this technique has been used to provide crucial information toward understanding reaction mechanisms in water.[44] The ESI mass spectra of

(41) Widegren, J. A.; Bennett, M. A.; Finke, R. G. *J. Am. Chem. Soc.* **2003**, *125*, 10301.
(42) Widegren, J. A.; Finke, R. G. *J. Mol. Catal. A* **2003**, *191*, 187.
(43) Hubbard, H. M.; Reynolds, C. A. *J. Am. Chem. Soc.* **1954**, *76*, 4300.
(44) Hayashi, H.; Ogo, S.; Abura, T.; Fukuzumi, S. *J. Am. Chem. Soc.* **2003**, *125*, 14266.

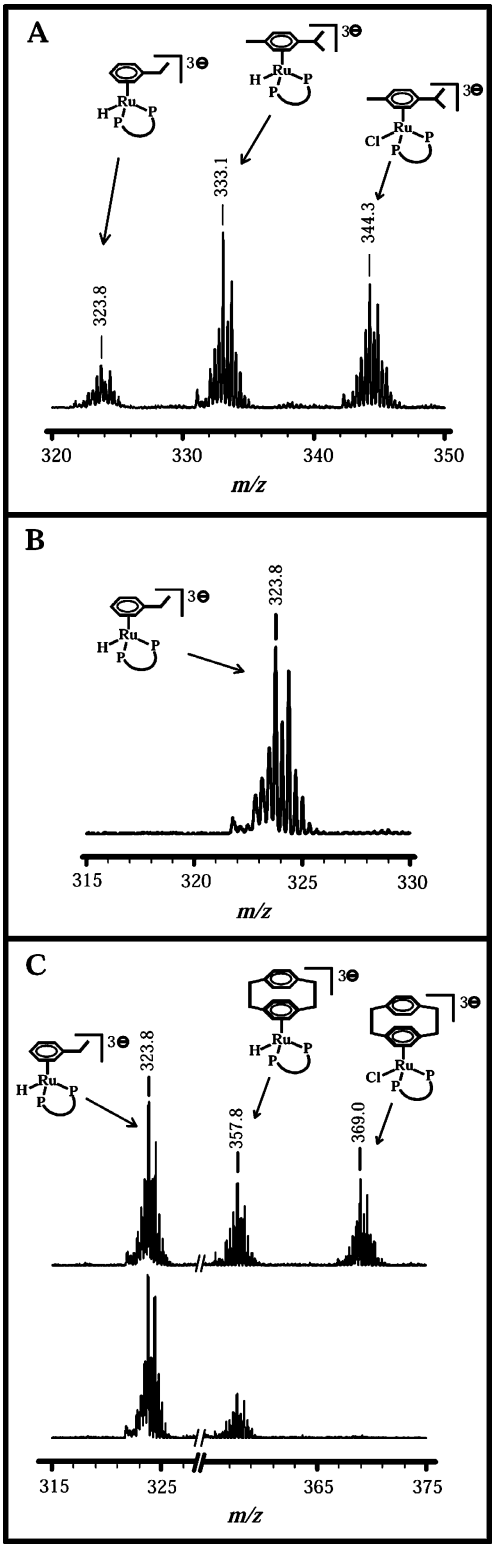


**Figure 5.** Species observed in the aqueous phase by ESI-MS after 2 h catalysis starting from precursors **4** (A), **5** (B), and **6** (C, top: 1 h, bottom: 2 h), P−P = dppbts. Conditions: 100 °C, $p(H_2) = 45$ bar, substrate/catalyst = 2000.

**4**−**6** are shown in Figure 5. The first feature to note is the formation of hydride species, which is accompanied by a decrease of the pH that was measured after the reaction was quenched. Combined, these observations demonstrate the heterolytic cleavage of dihydrogen. Activation of $H_2$ presumably takes place via a $\eta^2$-dihydrogen complex intermediate, as illustrated in Scheme 1 in the case of the *p*-cymene derivative. Due to the poor electron-donating properties of the ancillary ligands and the lower stability of the +IV oxidation state of ruthenium, the dihydrogen complex is preferred compared to the dihydride, although a dynamic equilibrium between these two species cannot be completely ruled out.

**Scheme 1. Heterolytic Activation of Dihydrogen by Complex 4**

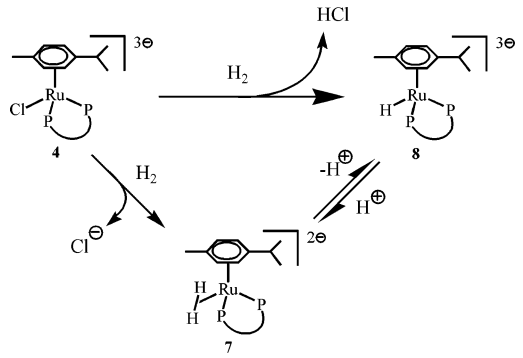


**Table 3. Hydrogenation of Styrene in Basic Aqueous Solution (pH 8)**[a]

| compound | conversion/% | selectivity/%[b] |
|---|---|---|
| **2** | 100 | 8 |
| **4** | <2 | |
| **5**[c] | 100 | 62 |
| **6** | 100 | 97 |
| **6**[d] | 10 | 100 |

[a] Conditions: 100 °C, $p(H_2) = 45$ bar, substrate/catalyst = 2000, 2 h. [b] Selectivity toward ethylbenzene, byproduct = ethylcyclohexane. [c] Decomposition of the complex. [d] Reaction time = 1 h.

The second feature to note from the ESI mass spectra is that arene exchange has taken place during catalysis. This point provides clues concerning the mechanism of coordination of the substrate and will be discussed below.

To establish the correlation between the activation of dihydrogen and the hydrogenation of styrene, the catalytic reactions were carried out in a basic buffer solution at pH 8. Conversion and selectivity for the different precursors are collected in Table 3. As previously reported for complex **1**, the reaction performed under basic conditions using **2** results in the hydrogenation of aromatics due to nanoparticle formation.[45] Thus, the selectivity for the reaction with **2** is very low since further hydrogenation to ethylcyclohexane takes place in basic solution. If nanoparticles were involved in the hydrogenation using the dppbts derivatives, the same behavior should be observed. This is the case for the benzene complex **5**, which decomposes to give black particles under these conditions and provides 38% of the fully hydrogenated product. In contrast, with the *p*-cymene analogue **4** the reaction is inhibited, with less than 2% conversion observed. ESI-MS analysis of the aqueous phase showed that **4** has been completely converted into the hydride **8**, and since no hydrogenation of the aromatic ring has taken place, the formation of nanoparticles seems unlikely. Furthermore, enhancement of the heterolytic cleavage of dihydrogen by a base

(45) Daguenet, C.; Dyson, P. J. *Catal. Commun.* **2003**, *4*, 153.

dramatically decreases the activity toward hydrogenation of the vinyl group. The hydride **8**, which displays a triplet at $\delta$ −11.4 ($^2J_{HP}$ = 35 Hz) in the $^1$H NMR spectrum, has been isolated and redissolved in pure water (pH 7) for catalysis, but still no hydrogenation was observed. Kalck et al. evaluated a related hydride ruthenium(II)-arene complex in diethyl ether, and although the conditions were different, they also noted that it was inactive toward alkene hydrogenation.[46] This is a rather unexpected result since activation of dihydrogen by ruthenium complexes is known to afford hydride compounds, which are believed to be active species for C=C bond hydrogenation.[18,19,47−53] In the present study, the active catalyst is thought to be the dihydrogen complex formed after the thermally induced dissociation of the chloride. Such active species have been previously proposed for alkene hydrogenation involving hydrogen transfer to the substrate directly from a molecular hydrogen complex.[20,54] Assuming that the same catalytic pathway occurs in a homogeneous organic phase, such as toluene, using precursors **1**−**3**, a dihydrogen complex as the active species is more likely than a monohydride complex since the heterolytic cleavage of $H_2$, in nonpolar organic solvents and in the absence of a base, is not favored. Attempts have been made to detect the dihydrogen complex **7** under a high pressure of $H_2$ using $^1$H NMR spectroscopy in methanol-$d_4$, but unfortunately, due to the high lability of the dihydrogen ligand in this complex, only the hydride **8** was detected even at low temperatures.

Concerning the [2.2]paracyclophane derivative, there is also a decrease of the activity under basic conditions, and after 1 h of reaction, analysis of the solution by ESI-MS reveals a large proportion of the $\eta^6$-[2.2]paracyclophane derivatives. Nevertheless after 2 h of reaction the same conversion as in pure water is measured and the arene exchange product [Ru(dppbts)($\eta^6$-ethylbenzene)H]$^{3-}$ dominates the ESI-MS spectrum. The rate of reaction is reduced in a basic medium, but catalytic hydrogenation can still take place without much decomposition, as indicated by the high selectivity. In relation to that, the [2.2]paracyclophane dihydrogen complex must be more stable than the *p*-cymene analogue, i.e., has a higher p$K_a$. A possible explanation would be that the lower electron density at the metal, in the case of the dihydrogen complex relative to the hydride, could be more easily stabilized by the [2.2]paracyclophane ligand compared to *p*-cymene due to an additional transition from orbitals of unbound deck $\pi$-character via the bound deck to the metal center.[55]

Recycling of the aqueous phase containing the ruthenium(II)-arene complexes has been carried out, and although the complexes are not lost to the organic phase and are well retained in the aqueous phase, catalytic activity is considerably reduced even after the second run. This reduction of activity is consistent with the previous results since most of the starting complex, [Ru($\eta^6$-arene)(dppbts)Cl]Na$_3$, is converted into hydride species, which have been shown to be inactive. The pH of the solution is decreased after the first run, presumably due to the heterolytic cleavage of dihydrogen, depicted in Scheme 1. The protonation/deprotonation equilibrium that takes place under high pressure of dihydrogen, in addition to ligand exchange equilibrium (see section on H/D isotope exchange), must be completely displaced toward the formation of the hydride after the gas is released. These acidic conditions, as discussed above, are not conducive to the catalytic hydrogenation of styrene.

**Arene Exchange.** As mentioned above, arene exchange takes place when catalyses are carried out with compounds **4**−**6**. In fact [Ru(dppbts)($\eta^6$-ethylbenzene)H]$^{3-}$ is observed to varying extents in the ESI mass spectra of each reaction (Figure 5). In addition, the $^1$H NMR spectrum of the aqueous phase after catalysis with **5**, for example, showed a triplet for the hydride signal at $\delta$ −11.20 with $J_{HP}$ = 34 Hz, and the chemical shifts corresponding to the coordinated ethylbenzene appeared at $\delta$ 0.62 (t, 3H), 1.99 (q, 2H), 5.80 (d, 2H), and 5.87−5.93 (m, 3H). Investigations on the exchange reaction have been conducted on **4** using slightly different conditions than those applied to the catalytic experiments. To see if the exchange could occur without catalytic hydrogenation of the vinyl group, ethylbenzene was used instead of styrene while the partial pressure of dihydrogen and the temperature were kept the same as for catalysis. The ESI mass spectrum of the reaction mixture showed the presence of **4** as well as the corresponding hydride, but no hydride resulting from arene exchange was observed. It must be noted that chloride complexes with an exchanged arene have not been detected after catalysis. In the same way, reaction of **4** with a mixture of styrene/ethylbenzene without pressurization with dihydrogen did not lead to any arene exchange. According to these results, both the substrate and the dihydrogen are required to induce arene exchange. In addition, the exchange must occur after the loss of chloride, namely, on the dihydrogen complex. Due to the strong *trans*-influence of hydride ligands, the labilization of the arene, generating an exchange reaction, could also occur on the complex [Ru(dppbts)($\eta^6$-arene)H]$^{3-}$. Therefore the same reactions have been carried out starting from compound **8**, but only traces of [Ru(dppbts)($\eta^6$-ethylbenzene)H]$^{3-}$ were detected. It can therefore be concluded that the exchange on complex **4** is facilitated during the catalytic hydrogenation of styrene and is taking place on the dihydrogen complex **7** through a labilization of the *p*-cymene ligand by the substrate. Moreover, the use of an aromatic cosolvent such as toluene in catalysis leads to the formation of [Ru(dppbts)($\eta^6$-toluene)H]$^{3-}$ in addition to the other species. Bennett and co-workers have previously described the labilization of coordinated naphthalene (a relatively labile arene ligand), in which two-electron donor ligands such as acetonitrile or phosphines can bind to the metal inducing a ring-slippage

(46) Hernandez, M.; Kalck, P. *J. Mol. Catal. A* **1997**, *116*, 131.
(47) Evans, D.; Osborn, J. A.; Jardine, F. H.; Wilkinson, G. *Nature* **1965**, *208*, 1203.
(48) Rose, D.; Gilbert, J. D.; Richardson, R. P.; Wilkinson, G. *J. Chem. Soc. A* **1969**, 2610.
(49) Ogata, I.; Iwata, R.; Ikeda, Y. *Tetrahedon Lett.* **1970**, *34*, 3011.
(50) Fahey, D. R. *J. Org. Chem.* **1973**, *38*, 3343.
(51) Iwata, R.; Ogata, I. *Tetrahedron* **1973**, *29*, 2753.
(52) Yi, C. S.; Lee, D. W.; He, Z.; Rheingold, A. L.; Lam, K.-C.; Concolino, T. E. *Organometallics* **2000**, *19*, 2909.
(53) Wiles, J. A.; Bergens, S. H.; Vanhessche, K. P. M.; Dobbs, D. A.; Rautenstrauch, V. *Angew. Chem., Int. Ed.* **2001**, *40* (5), 914.
(54) Kirss, R. U.; Eisenschmid, T. C.; Eisenberg, R. *J. Am. Chem. Soc.* **1988**, *110*, 8564.
(55) Swann, R. T.; Hanson, A. W.; Boelkelheide, V. *J. Am. Chem. Soc.* **1986**, *108*, 3324.

**Scheme 2. Proposed Mechanism of Styrene Hydrogenation Using 4, P−P = dppbts**

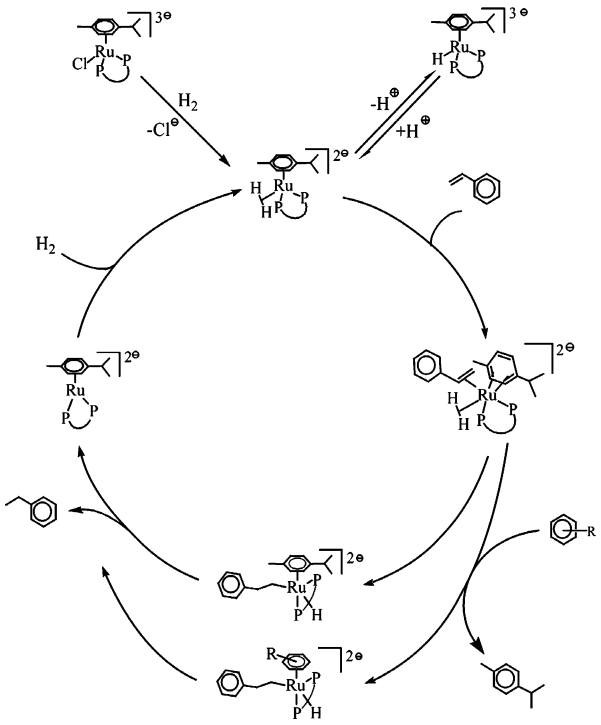

from $\eta^6$ to $\eta^4$ coordination mode, which is then followed by the substitution of the naphthalene by another arene.[56,57] Accordingly, in the present case, the alkene is the two-electron donor ligand inducing the arene exchange. Hence, a $\eta^4$ arene complex with a coordinated substrate can be postulated as an intermediate in the catalytic cycle proposed in Scheme 2. Species with a $\eta^6$ coordinated styrene have not been observed after hydrogenation even if the reaction is stopped before completion. Consequently, it is not unreasonable to assume that the binding of free styrene to the catalytic intermediate goes preferentially via the C=C bond, which undergoes hydrogenation, than via the aromatic ring. Mechanisms involving a ring-slippage to allow the coordination of an entering ligand (substrate or reactant) have already been suggested for transfer hydrogenation of ketones.[22,58] Assuming a $\eta^6$ to $\eta^4$ arene coordination shift as a step in the catalytic cycle, the higher activity of complex **6** compared to **4** can be rationalized by the geometry of the [2.2]paracyclophane ligand, with a nonplanar aromatic ring, being better suited to $\eta^4$ bonding.[55] The electronic nature of the [2.2]-paracyclophane ligand might also play a part in increasing catalytic activity. Indeed, the ease of reduction, related to the feasible $\eta^4$ coordination, and the ease of oxidation, due to the additional electronic donation from the unbound ring, might facilitate both oxidative addition and reductive elimination steps in catalytic cycles.[55,59]

The efficiency of arene exchange varies according to the precursor used, as is evident from the ESI mass spectra shown in Figure 5. The lability of the arene follows the series benzene > [2.2]paracyclophane > *p*-cymene. The greater lability of the benzene ligand, which can be displaced without addition of substrate, can be related to the lower stability of complex **5** observed under more drastic conditions (basic medium). When the catalytic hydrogenation is performed with vinylcyclohexane instead of styrene, no conversion is observed for the reactions with **4** and **6**, whereas complex **5** is active, but decomposes during catalysis because no aromatics are present that may coordinate to the metal. Since vinylcyclohexane is more crowded than styrene, its coordination to the metal center is difficult unless the coordinated arene is (partially) displaced, which appears to be the case with **5**. This test indicates that, for **4** and **6** at least, the aromatic ring (primary or exchanged) remains coordinated to ruthenium during the hydrogenation of styrene.

**H/D Isotope Exchange.** Catalytic isotope exchange between $H_2$ and $D_2O$ or $D_2$ and $H_2O$ by transition metal complexes is believed to take place via a $\eta^2$-coordinated dihydrogen.[21,60−63] Such dihydrogen complexes must have both a high kinetic acidity, to incorporate the other isotope by H/D exchange, and a great lability toward ligand dissociation, to allow the evolution of the gas. Recording the evolution of HD in a $H_2-D_2O$ mixture by $^1$H NMR spectroscopy can indirectly demonstrate the existence of a $\eta^2$-$H_2$ species. Following the procedure applied by Lau and co-workers,[21,62] a toluene-$d_8$ column was added over a solution of **5** in $D_2O$ and pressurized with 50 bar of $H_2$ in a sapphire NMR tube. After 20 h of heating at 80 °C, the $^1$H NMR spectrum of the organic phase was recorded. The spectrum displays a triplet at $\delta$ 4.47 with $J_{HD} = 42.7$ Hz, corresponding to HD (Figure S1 in the Supporting Information), indicating the presence of a $\eta^2$-$H_2$ intermediate.

The H/D isotope exchange process has also been investigated under conditions of catalytic hydrogenation of styrene. To study this process, **5**, which converts completely into the arene-exchanged hydride complex during catalysis, was used as precursor. The aqueous phase of each catalytic experiment, i.e., in $D_2-D_2O$, $D_2-H_2O$, $H_2-D_2O$, and $H_2-H_2O$, was analyzed by ESI-MS after the reaction (Figure 6). The gray band in Figure 6 represents one unit on the *m*/*z* scale, which corresponds to the difference of three units of molecular weight between the trianionic species [Ru(dppbts)($\eta^6$-$C_6H_5$-$CH_2CH_3$)H]$^{3-}$ and [Ru(dppbts)($\eta^6$-$C_6H_5CHDCH_2D$)D]$^{3-}$. Under the $D_2-H_2O$ and $H_2-D_2O$ conditions, the spectra obtained correspond to a mixture of partially deuterated products (Figure 6, B and C). Considering *M* as the mass of the fully hydrogenated compound, the relative intensities of the peaks for the experimental spectra (B and C) were fitted using a linear combination of the relative intensities of the simulated isotopic patterns for the species *M*, *M*+1, *M*+2, and *M*+3 in order to get an approximation of their proportions in the mixture. In

(56) Bennett, M. A.; Neumann, H.; Thomas, M.; Wang, X. *Organometallics* **1991**, *10*, 3237.
(57) Bennett, M. A.; Lu, Z.; Wang, X.; Bown, M.; Hockless, D. C. R. *J. Am. Chem. Soc.* **1998**, *120*, 10409.
(58) Ghebreyessus, K. Y.; Nelson, J. H. *J. Organomet. Chem.* **2003**, *669*, 48.
(59) Bond, A. M.; Dyson, P. J.; Humphrey, D. G.; Lazarev, G.; Suman, P. *J. Chem. Soc., Dalton Trans.* **1999**, 443.
(60) Collman, J. P.; Wagenknecht, P. S.; Hembre, R. T.; Lewis, N. S. *J. Am. Chem. Soc.* **1990**, *112*, 1294.
(61) Kubas, G. J.; Burns, C. J.; Khalsa, G. R. K.; Van Der Sluys, L. S.; Kiss, G.; Hoff, C. D. *Organometallics* **1992**, *11*, 3390.
(62) Lau, C.-P.; Cheng, L. *J. Mol. Catal.* **1993**, *84*, 39.
(63) Kovács, G.; Nádasdi, L.; Laurenczy, G.; Joó, F. *Green Chem.* **2003**, *5*, 213.

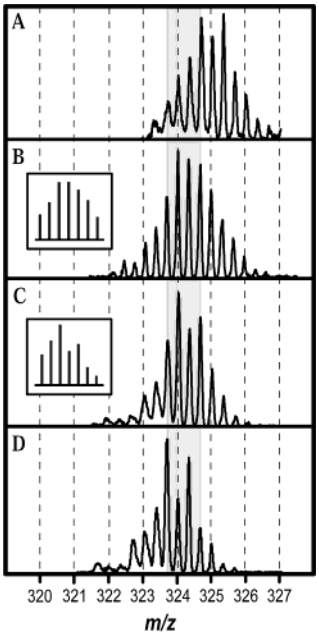


**Figure 6.** ESI-MS spectra of [H(D)Ru(dppbts)($\eta^6$-$C_6H_5$-$CH_2$(HD)$CH_3$($H_2$D))]$^{3-}$ formed during catalytic hydrogenation of styrene with **5** in (**A**) $D_2-D_2O$, (B) $D_2-H_2O$, (C) $H_2-D_2O$, and (D) $H_2-H_2O$. Reaction conditions: 100 °C, $p$($H_2$ or $D_2$) = 30 bar, 4 h. The frames correspond to calculated isotopic patterns for mixtures of products.

the $H_2-D_2O$ reaction, only two species corresponding to $M$ (17%) and $M+1$ (83%) are present. The latter must be the deuteride complex according to the $^1$H NMR spectrum, which shows a rather well-defined triplet at $\delta$ 0.57 and a quartet at $\delta$ 1.95 ($^3J_{HH}$ = 7.5 Hz) attributed to the fully hydrogenated ethyl group of the coordinated ethylbenzene. In contrast, the product distribution resulting from the reaction in $D_2-H_2O$ is more complicated, with a mixture of species of the three different masses $M+1$ (40%), $M+2$ (46%), and $M+3$ (14%), indicating that other compounds are present.

What is clear from these experiments is that the incorporation of hydrogen (or deuterium) from $H_2O$ (or $D_2O$) into styrene is more efficient with the $D_2-H_2O$ reactants than with $H_2-D_2O$. Under the latter conditions, the catalytic hydrogenation of styrene must take place faster on the $\eta^2$-$H_2$ complex than on the $\eta^2$-HD one and H/D exchange is only observable because the deuteride species is formed. Conversely, with the $D_2-H_2O$ reactants, the H/D exchange has an effect on the isotopic distribution in the coordinated ethylbenzene; the reaction must be slower on the $\eta^2$-$D_2$ complex than on the $\eta^2$-HD one, leading to incorporation of hydrogen into the substrate.

These data provide further evidence for an acid−base dynamic equilibrium between the dihydrogen and the hydride complexes. The kinetics and thermodynamics of this equilibrium, which have not been studied in this work, certainly play an important part in the catalytic process since the active species is believed to be the short-lived dihydrogen complex. Based on the results described herein, the mechanism illustrated in Scheme 2 is proposed.

The loss of the chloride ligand would generate from **4** a 16-electron complex, which might be stabilized by the formation of an aqua species, and leads to the active dihydrogen complex in equilibrium with the hydride. The dihydrogen species then enters the catalytic cycle by coordination of the substrate accompanied by a $\eta^6$ to $\eta^4$ ring-slippage, labilizing the arene and facilitating arene exchange. The dihydrogen is then cleaved and one H is added to the C=C bond to form a ruthenium(IV) alkyl hydride intermediate in which the arene coordinates in the usual $\eta^6$ mode. Reductive elimination of ethylbenzene would afford the 16-electron species that can re-enter the cycle by reaction with dihydrogen.

In conclusion, we have provided evidence that is not inconsistent with the existence of a dihydrogen complex in the catalytic hydrogenation of styrene using ruthenium(II)-arene precursors. The arene ligand may undergo exchange, but its loss is not a prerequisite for catalysis as in many reactions involving ruthenium(II)-arene precatalysts, which are finding ever-increasing applications in organic synthesis.

## Experimental Section

**General Procedures.** All organic solvents used were analytical grade. Deionized water was used for the compound preparation and doubly distilled water for the catalytic reactions. $RuCl_3 \cdot xH_2O$ (Apollo), diphenylphosphinomethane (dppm), diphenylphosphinoethane (dppe), diphenylphosphinopropane (dppp) (Acros Organics), 1,2-bis(di-4-sulfonatophenylphosphino)benzene (dppbts) tetrasodium salt (Strem Chemicals), hydrogen 45 (Carbagas), and deuterium 99.6% (Cambridge Isotope Laboratories Inc.) were used as received. The *p*-cymene, benzene, and [2.2]paracyclophane dimers, [$RuCl_2$($\eta^6$-arene)]$_2$, were prepared as previously described.[55,64,65] NMR spectra were recorded on either a Bruker Avance 200 or a Bruker Avance DPX 400 spectrometer. $^1$H and $^{13}$C chemical shifts were referenced to residual solvent resonances, and $^{31}$P chemical shifts were referenced to an external 85% aqueous solution of $H_3PO_4$. High gas pressure NMR experiments were carried out using sapphire NMR tubes.[38] ESI mass spectra were recorded on a Thermo Finnigan LCQ DECA XPPlus using conditions described previously.[24]

**Preparation of [($\eta^6$-*p*-Cymene)($\eta^2$-dppm)RuCl]Cl (1).** Compound **1** was prepared as reported earlier.[45] The tetrafluoroborate analogue of **1** was formed by anion exchange in an aqueous solution of **1** (ca. 10 mg in 20 mL) saturated with ammonium tetrafluoroborate (ca. 50 mg). The resulting yellow-white precipitate was washed with water and diethyl ether. Crystals suitable for X-ray analysis were grown by slow evaporation of acetone.

$^1$H NMR ($CDCl_3$) $\delta$ (ppm): 7.60−7.37 (m, 20H, C(Ph)*H*), 6.21 (d, $^3J_{HH}$ = 7 Hz, 2H, C*H*), 6.11 (d, $^3J_{HH}$ = 7 Hz, 2H, C*H*), 4.77 (dt, $^2J_{HH}$ = 15 Hz, $^2J_{HP}$ = 10 Hz, 1H, PC*H*HP), 4.55 (dt, $^2J_{HH}$ = 15 Hz, $^2J_{HP}$ = 10 Hz, 1H, PCHC*H*P), 2.48 (sept, $^3J_{HH}$ = 7 Hz, 1H, C*H*($CH_3$)$_2$), 1.52 (s, 3H, C$H_3$), 1.05 (d, $^3J_{HH}$ = 7 Hz, 6H, CH(C$H_3$)$_2$). $^{31}$P NMR ($CDCl_3$) $\delta$ (ppm): +0.44.

**Preparation of [($\eta^6$-*p*-Cymene)($\eta^2$-dppe)RuCl]Cl (2).** A suspension of the ruthenium *p*-cymene dimer (200 mg, 0.327 mmol) in ethanol (40 mL) was added to a solution of dppe (560 mg, 1.41 mmol) in ethanol (100 mL). The mixture was heated at 50 °C for ca. 20 h. The solution was cooled to room temperature, filtered, and concentrated to 2 mL. Addition of diethyl ether (ca. 15 mL) allows formation of a precipitate. The crude product was then washed with diethyl ether (15 mL), filtered, and dried to finally yield a yellow solid (337 mg, 73%). The tetrafluoroborate analogue was formed using the same method as for the dppm chelate described above. X-ray suitable

(64) Bennett, M. A.; Huang, T.-N.; Matheson, T. W.; Smith, A. K. *Inorg. Synth*. **1982**, *21*, 74.
(65) Zelonka, R. A.; Baird, M. C. *Can. J. Chem*. **1972**, *50*, 3063.

crystals of the tetrafluoroborate analogue were obtained by slow evaporation of an acetone solution.

$^1$H NMR ($CDCl_3$) $\delta$ (ppm): 7.73−7.23 (m, 20H, C(Ph)*H*), 6.10 (d, $^3J_{HH}$ = 6 Hz, 2H, C*H*), 6.01 (d, $^3J_{HH}$ = 6 Hz, 2H, C*H*), 2.92 (m, 2H, PC$H_2$), 2.48 (m, 2H, PC$H_2$), 2.32 (sept, $^3J_{HH}$ = 7 Hz, 1H, C$H$(C$H_3$)$_2$), 1.14 (s, 3H, C$H_3$), 0.78 (d, $^3J_{HH}$ = 7 Hz, 6H, CH(C$H_3$)$_2$). $^{31}$P NMR ($CDCl_3$) $\delta$ (ppm): +69.4.

**Preparation of [($\eta^6$-*p*-Cymene)($\eta^2$-dppp)RuCl]Cl (3).** A hot solution of ruthenium *p*-cymene dimer (100 mg, 0.164 mmol) in ethanol (30 mL) was added to a boiling solution of dppp (290 mg, 0.703 mmol) in ethanol (40 mL). The reaction mixture was stirred at reflux temperature for 4 h and then concentrated to ca. 2 mL. The residue was triturated in diethyl ether (15 mL) and the precipitate filtered and dried to yield a yellow-orange solid (145 mg, 60%).

$^1$H NMR ($CDCl_3$) $\delta$ (ppm): 7.66−7.25 (m, 20H, C(Ph)*H*), 6.18 (d, $^3J_{HH}$ = 6 Hz, 2H, C*H*), 5.79 (d, $^3J_{HH}$ = 6 Hz, 2H, C*H*), 3.11−3.03 (m, 2H, C$H_2$), 2.25−2.19 (m, 4H, PC$H_2$), 2.09 (sept, $^3J_{HH}$ = 7 Hz, 1H, C$H$(C$H_3$)$_2$), 1.55 (s, 3H, C$H_3$), 0.83 (d, $^3J_{HH}$ = 7 Hz, 6H, CH(C$H_3$)$_2$). $^{31}$P NMR ($CDCl_3$) $\delta$ (ppm): +23.0, +22.8.

**Preparation of [($\eta^6$-*p*-Cymene)($\eta^2$-dppbts)RuCl]$Na_3$ (4).** A suspension of the ruthenium *p*-cymene dimer (35 mg, 0.057 mmol) in ethanol (5 mL) was added to a solution of dppbts (130 mg, 0.15 mmol) in water (5 mL). The mixture was stirred at room temperature for 30 min and then concentrated to ca. 1 mL. Addition of ethanol leads to precipitation of the product, which was washed by decantation with ethanol and diethyl ether and then dried to yield a yellow-orange solid (100 mg, 80%).

Anal. Calcd for $RuC_{40}H_{34}S_4O_{12}P_2ClNa_3\cdot 4H_2O$: C, 40.91; H, 3.60. Found: C, 41.34; H, 3.69. $^1$H NMR ($CD_3OD$) $\delta$ (ppm): 8.07−7.23 (m, 20H, C(Ph)*H*), 6.27 (s, 4H, C*H*), 2.45 (sept, $^3J_{HH}$ = 7 Hz, 1H, C$H$(C$H_3$)$_2$), 1.37 (s, 3H, C$H_3$), 0.87 (d, $^3J_{HH}$ = 7 Hz, 6H, CH(C$H_3$)$_2$). $^{31}$P NMR ($CD_3OD$) $\delta$ (ppm): +67.1. ESI-MS negative ion: *m*/*z* 344 $[M]^{3-}$, 516 $[M + H]^{2-}$, 528 $[M + Na]^{2-}$.

**Preparation of [($\eta^6$-Benzene)($\eta^2$-dppbts)RuCl]$Na_3$ (5).** A suspension of the ruthenium benzene dimer (30 mg, 0.060 mmol) in ethanol (5 mL) was added to a solution of dppbts (130 mg, 0.15 mmol) in water (5 mL). The mixture was stirred at room temperature for ca. 20 min and then concentrated to 1−2 mL. Addition of ethanol leads to precipitation of the product, which was washed by decantation with ethanol and then dried to yield a yellow-orange solid (70 mg, 52%).

Anal. Calcd for $RuC_{36}H_{26}S_4O_{12}P_2ClNa_3\cdot 4H_2O$: C, 38.66; H, 3.06. Found: C, 39.16; 3.27. $^1$H NMR ($CD_3OD$) $\delta$ (ppm): 8.07−7.14 (m, 20H, C(Ph)*H*), 6.22 (s, 6H, C*H*). $^{31}$P NMR ($CD_3OD$) $\delta$ (ppm): +65.1. ESI-MS negative ion: *m*/*z* 326 $[M]^{3-}$, 489 $[M + H]^{2-}$, 500 $[M + Na]^{2-}$.

**Preparation of [($\eta^6$-*p*-Cyclophane)($\eta^2$-dppbts)RuCl]$Na_3$ (6).** A suspension of the ruthenium [2.2]paracyclophane dimer (30 mg, 0.039 mmol) in ethanol (4 mL) was added to a solution of dppbts (95 mg, 0.12 mmol) in water (4 mL). The mixture was stirred at room temperature for ca. 30 min, filtered, and concentrated to 1 mL. Addition of ethanol leads to precipitation of the product, which was washed by decantation with ethanol and then dried to yield a yellow-orange solid (46 mg, 47%). Anal. Calcd for $RuC_{46}H_{36}S_4O_{12}P_2ClNa_3\cdot 5H_2O$: C, 43.62; H, 3.66. Found: C, 43.28; 3.71. $^1$H NMR ($CD_3OD$) $\delta$ (ppm): 7.96−6.92 (m, 20H, C(Ph)*H*), 6.90 (s, 4H, C*H*), 5.21 (s, 4H, C*H*), 3.28−3.24 (m, 4H, C$H_2$), 2.94−2.90 (m, 4H, C$H_2$). $^{31}$P NMR ($CD_3OD$) $\delta$ (ppm): +72.9. ESI-MS negative ion: *m*/*z* 369 $[M]^{3-}$, 554 $[M + H]^{2-}$, 565 $[M + Na]^{2-}$.

**Preparation of [($\eta^6$-*p*-Cymene)($\eta^2$-dppbts)RuH]$Na_3$ (7).** In a stainless autoclave, [($\eta^6$-*p*-cymene)($\eta^2$-dppbts)RuCl]$Na_3\cdot 4H_2O$ (10 mg, 0.0085 mmol) was added to a 50 mM phosphate buffer pH 8 (2.5 mL). The system was pressurized at 45 bar with dihydrogen and heated to 100 °C for 2 h. The gray reaction mixture was concentrated under reduce pressure, extracted with methanol, and then filtered. The filtrate was evaporated to dryness to yield a light-yellow-gray solid (6 mg, 66%).

$^1$H NMR ($CD_3OD$) $\delta$ (ppm): 7.99−7.37 (m, 20H, C(Ph)*H*), 5.90 (d, $^3J_{HH}$ = 6.4 Hz, 2H, C*H*), 5.77 (d, $^3J_{HH}$ = 6.4 Hz, 2H, C*H*), 2.21 (sept, $^3J_{HH}$ = 7 Hz, 1H, C$H$(C$H_3$)$_2$), 1.76 (s, 3H, C$H_3$), 0.87 (d, $^3J_{HH}$ = 6.8 Hz, 6H, CH(C$H_3$)$_2$), −11.38 (t, $^2J_{HP}$ = 35 Hz, 1H, Ru*H*). $^{31}$P NMR ($CD_3OD$) $\delta$ (ppm): 78.0 (d, $^2J_{PH}$ = 35 Hz). ESI-MS negative ion: *m*/*z* 333 $[M]^{3-}$, 511 $[M + Na]^{2-}$.

**Catalysis.** All catalytic experiments were conducted using a home-built multicell autoclave at 100 °C pressurized with either hydrogen or deuterium. To each reaction vessel the catalyst (ca. $4 \times 10^{-3}$ mmol) and the substrate (1 mL) were weighted and the solvent (1.5 mL) was added via syringe. The catalytic runs were carried out using varying lengths of time and the percent conversions determined by GC analysis of the organic phase performed with a Varian Chrompack CP-3380 gas chromatograph. The mercury poisoning experiments were conducted in the same way with the addition of about 100 $\mu$L of Hg(0) to the reaction vessel.

**Data Analysis.** Conversions after catalysis were determined by integration of the corresponding peaks on the chromatograms using Varian software. Integrations of the NMR signals for the kinetics studied by high gas pressure NMR measurements were performed with a Levenberg−Marquard fitting procedure on the NMRICMA program working on a Matlab platform.[66] Initial rates were calculated from the parameters determined with a pseudo-first-order kinetics model by a least-squares fit of the data using Scientist for Windows.

**X-ray Characterization of 1·$BF_4$ and 2·$BF_4$.** Details about the crystals and their structure refinement are listed in Table 1, and relevant geometrical parameters, including bond lengths and angles are included in the figure captions (see Figures 1 and 2). Data collection for **1**·$BF_4$ was performed at room temperature on a mar345 IPDS and for **2**·$BF_4$ at 140 K on a four-circle goniometer having kappa geometry and equipped with an Oxford Diffraction KM4 Sapphire CCD. Data reduction was carried out on both data collections with CrysAlis RED, release 1.7.0.[67] Absorption corrections have been applied to both data sets. Structure solution and refinement as well as molecular graphics and geometrical calculations were performed for both structures with the SHELXTL software package, release 5.1.[68] The structures were refined using full-matrix least-squares on $F^2$ with all non-H atoms anisotropically defined. H atoms were placed in calculated positions using the "riding model". Some disorder (see Figure 1) has been encountered during the refinement of **1**·$BF_4$ and has been treated splitting the phenyl ring into two different orientations (named A and B), having the same occupancy factor and the same regular and fixed geometry.

**Acknowledgment.** We thank Novartis, the EPFL, and Swiss National Science Foundation for financial support.

**Supporting Information Available:** Crystallographic information for **1**·$BF_4$ and **2**·$BF_4$ in CIF format, 2D $^{13}$C−$^1$H NMR data for **4**−**6**, and Figure S1. This material is available free of charge via the Internet at http://pubs.acs.org.

OM049665Q

(66) Helm, L.; Borel, A. *NMRICMA 2.8*; Lausanne, Switzerland, 2001.

(67) *CrysAlis RED*, release 1.7.0; Oxford Diffraction Ltd.: Abingdon, Oxfordshire, UK, 2003.

(68) Sheldrick, G. M. *SHELXTL*; University of Göttingen: Germany, 1997; Bruker AXS, Inc., Madison, WI, 1997.